Wettability influence on the onset temperature of pool boiling: experimental evidence onto ultra-smooth surfaces.

B. BOURDON [(1)], E. BERTRAND [(1)], P. DI MARCO [(2)], M. MARENGO [(3,4)], R. RIOBOO [(1,5)] and J. DE CONINCK [(1)]*

[(1)] Laboratoire de Physique des Surfaces et des Interfaces, Université de Mons, Av. Maistriau, 19, B-7000 Mons (Belgium)

[(2)] Università di Pisa - DESTEC, largo L. Lazzarino, 1, 56122, Pisa (Italy)

[(3)] Department of Engineering, University of Bergamo, Viale Marconi 5, 24044 Dalmine (Italy)

[(4)] School of Computing, Engineering and Mathematics, University of Brighton, Brighton BN2 4GJ, United Kingdom

[(5)] Current address: Euro Heat Pipes, Rue de l'industrie, 24, B-1400 Nivelles (Belgium)

Corresponding author: Benoit Bourdon

Fax: +3265373881

Tel:+3265373883

E-mail: benoit.bourdon@umons.ac.be

Abstract

In this article we study systematically the effect of wettability on the onset of boiling on the same nanometrically smooth surface. By grafting different monolayers of molecules, we were able to explore the wettability from the equilibrium static contact angle, $\theta_0 = 0°$ to $\theta_0 = 110°$, without changing the surface topography. The superheat temperature at the onset of pool boiling was measured and eventually a non-classical trend of T_{ONB} as a function of wettability was observed. The nucleation site densities for the different grafting cases were also measured by image analysis. Moreover, we propose a novel theoretical interpretation to this phenomenon linking nucleation and the molecular diffusion coefficient. MD simulation results support this approach.

Keywords: pool boiling, wettability, surface treatment, superheat, heat transfer.

Table of content

1. Introduction

When a liquid is increasingly heated by a solid surface, boiling eventually occurs. While this phenomenon has been observed in everyday life and in industry, its control is of crucial importance. In particular, one of the most efficient cooling systems consists in using the phase change of a liquid and its latent heat to transfer heat from one point to another. The transfer of the heat from the solid surface to the fluid is a function of several parameters such as heat flux, materials properties, and the geometry of the interface. When increasing the heat flux, the solid temperature increases, and the heat transfer from the solid to the liquid passes through various regimes. The first regime is the single-phase convection, which has a moderate ability to transfer the heat, and at a given superheat, i.e., at a temperature higher than the equilibrium saturation temperature, the so-called onset of nucleate boiling (ONB) occurs. During nucleate boiling, the successive formation and, in gravity conditions, the departure of bubbles are observed to be associated with high heat fluxes. When the heat flux increases even more and reaches the so-called critical heat flux (CHF), an insulating gas layer covers the solid surface, which results in a strong and sudden increase of the solid temperature. In all cases, superheat, which is the difference between the temperature of the solid, T_w, and the saturation of the liquid, T_{sat}, is necessary to start boiling. This superheat is generally a function of the characteristics of the solid/liquid interface [1-3]. In particular, surface topography is of primary importance, since boiling is usually associated with the presence of cavities. While many studies have shown the effect of changing these material-related parameters on the boiling onset [4-19], using nano-coatings [16] or nano-fluids [20] for example, only a few have managed to decouple the surface structure with other effects more linked to the chemical properties of surface, such as the surface wettability [21-24]. A recent review of the influence of topography and wettability effects in pool boiling has been done by Cheng et al [25]. Recently, using highly polished metallic surfaces, we have shown [26] that roughness amplitudes as low as a few nanometers can induce changes in the necessary superheat to achieve boiling. To decouple topographical effects (with their inherent complexity of characterization) from wettability, it is necessary to use even smoother surfaces such as glass or silicon wafers. The effect of wettability has already been shown using water on ungrafted glass plates (hydrophilic) and grafted octadecyltrichlorosilane (OTS) (hydrophobic) plates [27]. In

such a case, the contact angle is null for a hydrophilic surface while, for a hydrophobic surface, it is about 115° for the advancing contact angle and 95° for the receding contact angle. The ONB superheat is significantly lower (more than 18K) when using a hydrophobic surface compared to a hydrophilic one. More recently, Jo et al. [28] studied the heterogeneous nucleation on ideally smooth surface. They have found that their results did not match with classical nucleation theories. They thus have adapted a new model based on the thermal boundary layer. Their model includes the kinetic dynamics of the superheated liquid and the thermodynamic stability of the generated vapor, inside three different thermal boundary layers.

In this paper the surface wettability was changed by grafting different monolayers on the same ultrasmooth surface, without modifying its topography. A non-linear decrease of the superheat temperature at the onset of boiling has been observed for increasing contact angles. Moreover, this behavior cannot be predicted by classical nucleation theories, but also by Jo et al. model's [28]. The nucleation site density was also estimated by measuring the number of bubbles over the different treated surfaces [29-31]. These results can be linked at least qualitatively to a molecular diffusion coefficient, estimated by molecular dynamic (MD) simulations. The use of MD simulations to describe the mobility of the liquid molecules in the vicinity of the surface offers a novel theoretical approach to the nucleation phenomenon.

2. Experimental methods

2.1. Materials and surface treatment

Following the goal of measuring the isolated effect of the wettability on the onset of nucleate boiling, possible roughness contribution has been minimized as much as possible. For that, we used special glass surfaces (float glass; Oedenkoven Fr S.A.), which are very smooth. A 3D picture and a topography profile of the surface acquired by AFM is shown on Figure 1. The main roughness parameters are presented in Table 1. Moreover, glass was chosen because of its strength to prevent any damage on the surface during boiling in contrast to metallic surfaces [26] and for its sturdiness compared to silicon wafers. Milli-Q water was used during the boiling experiments. Several silanes

were used to modify the wettability of the glass substrate by chemical grafting of self-assembling monolayers (SAM).

Octadecyltrichlorosilane (OTS) was purchased from Sigma-Aldrich (Germany), 2-[Methoxy-(polyethyleneoxy)propyl]-trimethoxysilane (MPEGPTMS) and 11-acetoxyundecyltriethoxysilane (AcOUTES) were purchased from Gelest, Inc. (USA). All chemicals were used without further purification. Each glass surface was cleaned and then grafted with a specific silane. The cleaning and grafting procedures have been optimized for MPEGPTMS [32], OTS [33,34] and AcOUTES [35] surfaces.

The non-grafted surface was cleaned with a piranha solution and rinsed abundantly with Milli-Q water. After the cleaning procedure, the surface becomes super-hydrophilic. This means that when we deposit the drop of water on the surface, a thin film of water is rapidly created and it is impossible to measure any non-negligible contact angle (i.e. $\theta_{adv.} = \theta_{rec.} = 0°$).

Insert Figure 1

2.2. Experimental setup and boiling procedure

We characterize the boiling behavior of the various substrates by recording the temperature at the onset of boiling and visualizing the appearance of bubbles on the surface using a high-speed camera (HCC-1000, VossKühler GmbH, Germany). The details of the experimental setup can be found in a previous paper [27] and are summarized here.

Figure 2 presents a schematic of the chamber where boiling on the surface is activated. The surface to be tested, a glass square plate of 45 mm wide and 1 mm thick, is encapsulated in a chamber in which vacuum has been performed before filling with boiled water. The vacuum achievement (30 mbars) obtained ensures a low level of dissolved air in the water [36]. Pressure is adjusted with a controller, and experiments are performed at atmospheric pressure; a bellows allows for dilatation of the working fluid during the experiment. A heater (ceramic cartridge, Acim Jouanin, 175 watts) is put in contact with the center part (20 mm diameter) of the back side of the glass plate using a spring. Between the heater and the plate, a heat-flux meter (Captec, France) enables the direct measurement of the heat flux; the thermal contact among various components is improved by using a conductive paste (RS, Heat Sink Compound Plus). The heating cartridge is insulated using Teflon. To compensate for possible thermal leakage, additional heaters are placed inside the chamber and on the aluminum walls of the chamber. The water in the chamber is maintained as close as possible to the saturation temperature by using these heaters, K-thermocouples in the chamber, and a PID controller.

Insert Figure 2

3. Results and discussion

Table 2 presents the various wettabilities obtained with the different surface treatments (cleaning only, and cleaning followed by the self-assembling of various silane monolayers). The low difference between values before and after boiling shows that grafting is of good quality. Moreover, the hysteresis of contact angles on glass surface is compatible with literature data [32-35].

The complete boiling curves are reported and discussed in Appendix 1. In this paper we focus mostly on the surface superheat at which the first bubbles are appearing versus the wettability of the solid surface, which is plotted vs. the surface wettability in Figure 3. In this figure, the wettability presented (angle θ_0) is calculated using the mean value of the four measured values of the advancing and receding static contact angles before and after boiling for each surface. In the same way, the error bars are estimated using the maximum of the hysteresis of the static contact angles (between the one before and the one after boiling) for each surface. The influence of the wettability is clear: Increasing the wettability on a very smooth, non-conductive surface results in an increase of the necessary superheat to get the appearance of the first bubble. The relationship is clearly not linear. If one would consider the theoretical case of perfect wetting (null static contact angles) with heterogeneous nucleation on an ideal smooth surface, an additional data point has to be added at $\Delta T \approx 200K$ [37].Such a superheat is predicted by the classic heterogeneous nucleation theories without surface cavities, based on the thermodynamic calculations of the difference in terms of free energy; these theories are fully described in Carey's book [37]. In boiling experimentations, the systems used are far from ideal one. Even if the water and the chamber are well degassed, a small amount of air remains in the liquid. We have measured the partial pressure of air inside the chamber by subtracting the saturated pressure of the water from the total pressure of the chamber [36]. The estimated maximum partial pressure of air in the chamber during boiling experiments was about 2.1 kPa. Moreover, the values reported in Figure 3 are of the same order of magnitude than other experimental works that have been presented in [28]. In this article, Jo et al. experimentally demonstrate that there is a decrease of the superheat needed to have boiling when the wettability of the surface is decreased. They predict theoretically the bubble nucleation condition by considering kinetic dynamics of water molecules and thermal equilibrium of the instantly generated bubble nucleus within three different boundary layer sizes. They also compare their predictions of the required superheat for the thermal equilibrium with two other works in literature [38,39] and show that the experimental results can be predicted by their model. Noteworthy, by comparing the R_a parameter, in all of these works, the smoothest surface used is at least two times rougher than in the

present work. Moreover, the roughness of the samples is changing when the wettability of the surfaces is modified. Jo et al. did not mentioned the contact angle hysteresis of their substrates and its possible role. Nevertheless if we put our results in terms of superheat on their prediction graph (Figure 9 in Appendix 1), we can see that only two of our four points are inside their prediction curve. The OTS case is in the "Not Activated" area while the non-grafted case is completely out of the range of the predicted superheat.

Finally, in the present article, we are able to show a trend (Figure 3) for the superheat needed to get boiling for a wide range of wettabilities, without modifying the surface topography by surface treatments. These results, until now and to the best of our knowledge, have never been presented and cannot be predicted by any theory. To check the repeatability of the experiments, and also to experimentally point out the fact that there is no preferential nucleation site over the surfaces (no cavities), we have visualized three times the location of the first bubble over the surface. We have realized that the first bubble appeared each time at a different location supporting the fact that only the wettability is acting on the boiling onset and no deterministic point linked to a surface heterogeneity is generating the bubble onset.

Insert Figure 3

Insert Figure 4

The upper part of Figure 4 shows the different boiling behavior between the AcOUTES (left) and the OTS (right) treatments at the same heat flux (12 kW/m^2). For the OTS case, bubbles nearly cover the entire heated surface; however, in the AcOUTES case, only a few bubbles are present. This means that there is an important proliferation in the number of nucleation sites passing from a nearly hydrophobic surface ($\theta_0 \approx 75°$) to a hydrophobic one ($\theta_0 \approx 105°$). The bottom part of this figure represents the quantification in terms of the number of nucleation sites per unit area (left) and vapor volume flux (right) at this heat flux for the three grafted surfaces (OTS, AcOUTES, and MPEGPTMS). The nucleation site density (bottom left) is in fact the mean number of bubbles

present on the surface. The error bars are the standard deviations. The vapor volume flux is calculated by an estimation of the detached bubble volume per time unit. The measure of the volume has been made by estimating the size of the bubbles, considering an axial symmetry. The error bars are estimated by the error on the X and Y pixels on the images. The bubbles are considered to be spherical. The non-grafted case is not represented because no bubbles were visualized at this level of heat flux. Finally the two graphs in Figure 4 show the same exponential growing trend in function of the contact angle. One can see that there is still a difference passing from a hydrophilic case to a hydrophobic one. This behavior, to the best of our knowledge, has never been studied in the literature and is not described by classical nucleation theories.

From these observations, we can conclude that there are more nucleation points on top of a hydrophobic surface than on a hydrophilic surface. Moreover, from the topography of our surfaces represented on Figure 1, and from the above-mentioned random location of nucleation sites in consecutive experiments, we can assume that the nucleation sites are not due to the cavities present over the substrate. Indeed, if we calculate the theoretical critical radius of nucleation, which is given by $r_c = \frac{2\sigma_{lv}}{P_{sat}(T_l)\exp\left[\frac{v_l\left(P_l - P_{sat}(T_l)\right)}{RT_l}\right] - P_l}$ (details in Carey's book [37]), we find a critical radius value of 9 µm for a superheat of about 3K (which corresponds to the most hydrophobic case) and a critical radius value of 1 µm for a superheat of about 20K (which corresponds to the most hydrophilic case). These values are of course much higher than the cavity size present over our surfaces (Figure 1).

How can we explain this new finding? The relative low values of the superheat at the onset of nucleate boiling is partially explained by the presence of nanobubbles over the surface. Indeed, it has been shown [41] that air nanobubbles are always present over hydrophobic surfaces and that it is possible that they remain on the surface even after one hour of degassing. No bubbles are detected over hydrophilic surfaces, even if checked at room temperature [41]. In the present case, the presence of such nanosystems is linked to the presence of both vapour nanobubbles and of air nanobubbles. Eventually the liquid close to the surface is superheated, i.e in a thermodynamical condition where it is possible to create vapor nanobubbles. These nanobubbles are usually unstable,

i.e. there is a statistical phenomenon of evaporation and condensation, but, in presence of an interface with chemical heterogeneities, they tend to settle on the surface with a higher probability to become stable and remain attached to the surface. Considering the air nanobubbles, there is a contact angle hysteresis on all surfaces we used, and the contact angles for the most hydrophilic case (after boiling experiment) are about 9° and 30° for the receding and advancing contact angles, respectively, which is in turn very similar to the MPEGPTMS case. The contact angle hysteresis is related to pinning [42] and therefore linked to the bubble liquid/air interfaces mobility on and from the surface. Therefore in our case we cannot exclude the presence of air nanobubbles even on hydrophilic surfaces. Moreover, we have measured the partial pressure of air inside the chamber and, from the Henry's law, we know that there is still a minimum quantity of air dissolved in the water (the estimated maximum partial pressure of air in the chamber during boiling experiments was about 2.1 kPa). This dissolved gas, by diffusion, will be also attached on the chemical heterogeneities of the surface, acting as nucleation sites and thus leading to the small superheat temperature at the onset of boiling, even on hydrophilic smooth surfaces.

If we look now at the molecular level, how we can assume that the bubble nucleation starts with a nanobubble of air in contact with the solid surface? The growth of this bubble will be due to the incorporation of water molecules in the gas phase and will be limited by the mechanisms controlling the mobility of the corresponding phase line. As known, this contact line will be subject to pinning (contact angle hysteresis) and to some dynamics. For a low viscosity liquid such as water, the dynamics is well described by the molecular kinetic theory [40], which links the corresponding speed of displacement to the mobility of molecules in contact with the surface.

Moreover, the water molecules move with a speed related to the temperature. In the vicinity of the wall container (the heat source), it is expected that the water molecules will move faster than in the liquid bulk. However, it seems natural to expect that the nucleation points will be directly related to that mobility. Indeed, a nucleation point is an assembly of high-speed water molecules that will be well separated from each other during a nano-gas phase. The mobility of molecules can be described by the diffusion constant. The previous observations are thus related to an increase of the diffusion

constant versus the value of the contact angle. We know that the diffusion constant will increase with temperature.

Is that also the case with wettability? To check this idea, we have performed large-scale molecular dynamics simulations. Our molecular dynamics algorithm and interactions used in this study are standard except that the fluid is made of chains of Lennard-Jones atoms to control the viscosity of the liquid. In this way, we attempt to come closer to the experiments. The basic interaction between pairs of atoms is of the Lennard-Jones type:

$$V_{ij}(r) = C_{ij}\left(\left(\frac{\sigma}{r}\right)^{12} - \left(\frac{\sigma}{r}\right)^{6}\right)$$

Where i and j represent solid or fluid atoms, and the fluid atoms are grouped into chains of length 8 with the additional pairwise (confining) potential:

$$U(r) = A\,\frac{r}{\sigma^6}$$

between adjoining atoms. Aside from the issue of molecular size, the chain structure has the effect of strongly reducing the volatility of the fluid so as to bring the simulation closer to experiments. The substrate is a lattice made of one layer of face-centered cubic (fcc) unit cells, and of which an atom of mass 50 is at each site (so as to have comparable timescales for the atomic motion in fluid and solid). For computational convenience, the tail of the potentials are cut off at $r_c = 2.5$, in units of the fluid core size. Given the potential, the motion follows from integrating Newton's equations, using a fifth-order predictor-corrector algorithm. In the remainder of the section, we non-dimensionalize by using σ, ε, and the fluid monomer mass as the units of distance, energy, and mass, respectively. This model is simplistic in terms of interactions, but is self-consistent in terms of physics.

The diffusion coefficient is obtained by measuring the mean square displacement of atoms over long period of times:

$$D_x = \frac{1}{2}\lim_{t\to\infty}\frac{d}{dt}\langle\sum\left(x_i(t) - x_i(t_0)\right)^2\rangle$$

Where $x_i(t_0)$ is the x position of atom i at starting time t_0, and $x_i(t)$ its position at time t. The brackets < > stand for the average over several starting times. More details about the system can be found in [40], where a detailed study of wettability has been performed. For instance, it has been shown that there is a direct link between the amplitude of interaction C and the static contact angle Θ_0.

For the same systems, it has been shown that the density of the liquid in the vicinity of the wall is also affected by the coupling C. Here, we have studied the values of the diffusion constants in the liquid, close to the wall for a fixed temperature. The results are given in Figure 5.

Insert Figure 5

Moreover, if we take the diffusion coefficient in the vicinity of the solid surface from [40] corresponding to comparable static contact angles in our experiments, we are able to plot those values on the graph representing the number of nucleation sites versus the contact angle at a given heat flux (bottom left of Figure 4). This leads to Figure 6 where we can see that the trend is compatible with our experiments, strengthening the link between the mobility of the molecules very close to the surface and the nucleation site density over different surface wettabilities.

Insert Figure 6

This clearly shows that the considered molecules are much more mobile in the vicinity of the wall whenever the static contact angle Θ_0 is large, in agreement with the experiments described in this paper. Of course, the agreement here is purely qualitative, since we are unable to simulate in details the behavior of real water molecules. But nevertheless, we believe that these results are going in the right direction and will help to build a future predictive theory.

4. Conclusions

Pool boiling experiments of water on smooth glass surfaces in stationary conditions were performed. The wettability was changed by grafting different monolayers on the surface. In this way, the wettability was modified without changing the roughness of the surface. We studied four different cases : (1) a non-grafted case, which has 0° contact angles (CA) before boiling; (2) an MPEGPTMS

299 case, which has about 33° CA; a AcOUTES case, which has about 70° CA; and an OTS case, which
300 is the most hydrophobic one and has about 102° CA. The boiling curves have been measured for
301 each case, and the temperature of the surface at the onset of boiling has been recorded. We have
302 observed a non-linear decrease of the superheat temperature at the onset of boiling decreasing the
303 wettability of the surface. We have also quantified the nucleation site density and the vapor volume
304 flux at a given heat flux for each case. Once more, the trend is not linear with the wettability of the
305 substrate, showing a big jump in passing from a hydrophilic surface to a hydrophobic one. An
306 explanation for this property is given in terms of molecular diffusion constant. In fact, for liquid
307 molecules in the vicinity of a solid wall, we have shown, using MD simulations, that the diffusion
308 constant is larger when the wettability is poor. The trend of diffusion coefficient with static contact
309 angle shows a nonlinear trend qualitatively similar to that of nucleation site density, which allows
310 inferring a link between these two quantities. On the other hand, with a larger diffusion constant, we
311 can expect a larger mobility and thus a larger probability to form a nanobubble of gas. This is in
312 qualitative agreement with our experimental observations. The results are useful for a wide set of
313 present and future applications, since the enhancement of boiling can be useful for microfluidic
314 evaporators, such as in micro- and nanorefrigerators, micro-HVAC systems, thermalized bacteria
315 detectors, and micro heat pipes.

316 **5. Acknowledgments**

317 Special thanks are due to A. Tomsia for his help during the preparation of the manuscript and to
318 Reyhan Sevkan for her help in the preparation of the surfaces. Benoît Bourdon is grateful to the
319 Belgian National Fund for Scientific Research (FRS-FNRS) for a FRIA doctoral grant. This research
320 has been partially funded by the Interuniversity Attraction Poles Programme (IAP 7/38
321 MicroMAST) initiated by the Belgian Science Policy Office, the Region Wallonne, and the FNRS.
322 The work was also carried on with the partial support of the PRIN 2009 project – Ministry of
323 University and Research, Italy.

324

Appendix 1

Figure 7 represents the boiling curve recorded for each surface treatment. The error bars correspond to the standard deviation calculated on at least three measurements. We can see that only the most hydrophobic case (OTS on the graph) shows a change in the slope of the boiling curve. The three other curves shows a linear behavior. We interpret this result by the fact that the thermal conductivity of the glass surface is too low and the boiling area is too small to record any local cooling of the surface from the bottom of it (indeed, the thermocouples are situated below the glass surface).

Insert Figure 7

Figure 8 represents the heat transfer coefficient (HTC) versus the heat flux for each surface treatment. Again, we observe a linear behavior of the curves corresponding to the three more hydrophilic treatment. There is a jump in the HTC only in the case of the OTS treatment, where the boiling is fully developed over the entire surface.

Insert Figure 8

Figure 9 represents a comparison of the predicted superheats (Jo et al. [28]) as a function of contact angle for different thermal boundary layer thicknesses with different experiments. As we can see, the superheat measured in this study cannot be predicted by their model. Our most hydrophobic case (OTS case) is located in the “Not Activated” area of the graph and our most hydrophilic case (not grafted case) is far from the predicted superheat.

Insert Figure 9

6. REFERENCES

1. M. Mann, K. Stephan, P. Stephan, Influence of heat conduction in the wall on nucleate boiling heat transfer, International Journal of Heat and Mass Transfer 43 (2000) 2193–2203.

2. I.L. Pioro, W. Rohsenow, S.S. Doerffer, Nucleate pool-boiling heat transfer. I: review of parametric effects of boiling surface, International Journal of Heat and Mass Transfer 47 (2004) 5033–5044.

3. H.T. Phan, R. Bertossi, N. Caney, P. Marty, S. Colasson, A model to predict the effect of surface wettability on critical heat flux, International Communication of Heat and Mass Transfer 39 (2012) 1500–1504.

4. J.Y. Lee, M.H. Kim, M. Kaviany, S.Y. Son, Bubble nucleation in microchannel flow boiling using single artificial cavity, International Journal of Heat and Mass Transfer 54 (2011) 5139–5148.

5. C. Hutter, D.B.R. Kenning, K. Sefiane, T.G. Karayiannis, H. Lin, G. Cummins, A.J. Walton, Experimental pool boiling investigations of FC-72 on silicon with artificial cavities and integrated temperature microsensors, Experimental Thermal and Fluid Science 34 (2010) 422-433.

6. C. Hutter, K. Sefiane, T.G. Karayiannis, A.J. Walton, R.A. Nelson, D.B.R. Kenning, Nucleation site interaction between artificial cavities during nucleate pool boiling on silicon with integrated micro-heater and temperature micro-sensors, International Journal of Heat and Mass Transfer 55 (2012) 2769–2778.

7. P. Papon, J. Leblond, P.H.E. Meijer, The physics of phase transitions, second ed., Springer-Verlag, Berlin, 2006, pp. 35-51.

8. H. Honda, J.J. Wei, Enhanced boiling heat transfer from electronic components by use of surface microstructures, Experimental Thermal and Fluid Science 28 (2004) 159-169.

9. L. Dong, X. Quan, P. Cheng, An analysis of surface-microstructures effects on heterogeneous nucleation in pool boiling, International Journal of Heat and Mass Transfer 55 (2012) 4376–4384.

10. T.G. Theofanous, J.P. Tu, A.T. Dinh, T.N. Dinh, The boiling crisis phenomenon Part I: nucleation and nucleate boiling heat transfer, Experimental Thermal and Fluid Science 26 (2002) 775-792.

11. S. Vemuri, K.J. Kim, Pool boiling of saturated FC-72 on nano-porous surface, International Communication of Heat and Mass Transfer 32 (2005) 27–31.

12. T. Chen, J.F. Klausner, S.V. Garimella, J.N. Chung, Subcooled boiling incipience on a highly smooth microheater, International Journal of Heat and Mass Transfer 49 (2006) 4399–4406.

13. Y. Nam, J. Wu, G. Warrier, Y.S. Ju, Experimental and numerical study of single bubble dynamics on a hydrophobic surface, Journal of Heat Transfer - Transactions of the ASME 31 (2009) 121004.

14. S. Kakaç, Boilers, Evaporators, and Condensers; Wiley, New-York, 1991.

15. A.E. Bergles, W.M. Rohsenow, The determination of forced-convection surface-boiling heat transfer, Journal of Heat Transfer 86 (1964) 365-370.

16. H.T. Phan, N. Caney, P. Marty, S. Colasson, J. Gavillet, Surface wettability control by nanocoating: The effects on pool boiling heat transfer and nucleation mechanism, International Journal of Heat and Mass Transfer 52 (2009) 5459–5471.

17. A.R. Betz, J. Xu, H. Qiu, D. Attinger, Do surfaces with mixed hydrophilic and hydrophobic areas enhance pool boiling?, Applied Physics Letters 97 (2010) 141909.

18. Z. Yao, Y.W. Lu, S.G. Kandlikar, Effects of nanowire height on pool boiling performance of water on silicon chips, International Journal of Thermal Sciences 50 (2011) 2084–2090.

19. H.J. Jo, H.S. Ahn, S.H. Kang, M.H. Kim, A study of nucleate boiling heat transfer on hydrophilic, hydrophobic and heterogeneous wetting surfaces, International Journal of Heat and Mass Transfer 54 (2011) 5643–5652.

20. S.J. Kim, I.C. Bang, J. Buongiorno, L.W. Hu, Surface wettability change during pool boiling of nanofluids and its effect on critical heat flux, International journal of heat and mass transfer 50 (2007) 4105-4116.

21. O.W. Thomas, R.E. Cavicchi, M.J. Tarlov, Effect of surface wettability on fast transient microboiling behavior, Langmuir 19 (2003) 6168-6177.

22. K.M. Balss, C.T. Avedisian, R.E. Cavicchi, M.J. Tarlov, Nanosecond imaging of microboiling behavior on pulsed-heated Au films modified with hydrophilic and hydrophobic self-assembled monolayers, Langmuir 21 (2005) 10459-10467.

23. R. Rioboo, M. Marengo, S. Dall'Olio, M. Voué, J. De Coninck, An innovative method to control the incipient flow boiling through grafted surfaces with chemical patterns, Langmuir 25 (2009) 6005-6009.

24. C. Choi, J.S. Shin, D.I. Yu, M.W. Kim, Flow boiling behaviors in hydrophilic and hydrophobic microchannels, Experimental Thermal and Fluid Science 35 (2011) 816-824.

25. P. Cheng, X.J. Quan, S. Gong, L.N. Dong, F.J. Hong, Recent studies on surface roughness and wettability effects in pool boiling, Proceedings of the 15th International Heat Transfer Conference, IHTC-15, August 10-15, 2014, Kyoto, Japan.

26. B. Bourdon, R. Rioboo, M. Marengo, E. Gosselin, J. De Coninck, Influence of the wettability on the boiling onset, Langmuir 28 (2012) 1618-1624.

27. B. Bourdon, P. Di Marco, R. Rioboo, M. Marengo, J. De Coninck, Enhancing the onset of pool boiling by wettability modification on nanometrically smooth surfaces, International Communication in Heat and Mass Transfer 45 (2013) 11-15.

28. H. Jo, M. Kaviany, S.H. Kim, M.H. Kim, Heterogeneous bubble nucleation on ideally-smooth horizontal heated surface, International Journal of Heat and Mass Transfer 71 (2014) 149-157.

29. N. Basu, G.R. Warrier, V.K. Dhir, Onset of nucleate boiling and active nucleation site density during subcooled flow boiling, Journal of Heat Transfer (2002), Vol 174 / 717.

30. G. Barthau, Active nucleation site density and pool boiling heat transfer- an experimental study, International Journal of Heat and Mass Transfer (1992), Vol. 35, No 2, pp 271-278.

31. R.J. Benjamin, A.R. Balakrishnan, Nucleation site density in pool boiling of saturated pure liquids: effects of surface microroughness and surface and liquid physical properties, Experimental Thermal and Fluid Science 1997; 15:32-42.

32. Papra, A.; Gadegaard, N.; Larsen, N.B. *Langmuir* **2001**, *17*, 1457-1460.

33. S.R. Wasserman, Y.T. Tao, G.M. Whitesides, Structure and reactivity of alkylsiloxane monolayers formed by reaction of alkyltrichlorosilanes on silicon substrates, Langmuir 5 (1989) 1074-1087.

34. R. Rioboo, M. Voué, M.H. Adão, J. Conti, A. Vaillant, D. Seveno, J. De Coninck, Drop impact on soft surfaces: beyond the static contact angles, Langmuir 26 (2010) 4873-4879.

35. M. K. Chaudhury, Surface free energies of alkylsiloxane monolayers supported on elastomeric polydimethylsiloxanes, Contact Angle, Wettability and Adhesion, 691-697, Ed. K. L. Mittal.

36. C. D. Henry, J. Kim, B. Chamberlain, Heater size and heater aspect ratio effects on subcooled pool boiling heat transfer in low-G, Third International Symposium on Two-Phase Flow Modeling and Experimentation, Pisa, 22-24 September 2004.

37. Van P. Carey, Liquid-Vapor Phase-Change Phenomena, Second Edition, 2008, Taylor & Francis Group, LLC.

38. H.J. Jo, S.H. Kim, M.H. Kim, Nucleate boiling performance on nano/microstructures with different wetting surfaces, Nanoscale Res. Lett. 7 (2012) 1-9.

443 39. Y. Takata, S. Hidaka, T. Uraguchi, Boiling feature on a super water-repellent surface, Heat
444 Transfer Eng. 27 (2006) 25-30.

445 40. E. Bertrand, T. Blake, J. De Coninck, Influence of solid-liquid interactions on dynamic wetting:
446 a molecular dynamics study, Journal of Physics Condensed Matter 21 (2009), 464124.

447 41. X.H. Zhang, G. Li, N. Maeda, J. Hu, Removal of induced nanobubbles from water/graphite
448 interfaces by partial degassing, Langmuir (2006), 22, 9238-9243.

449 42. P. Collet, J. De Coninck, F. Dunlop et A. Reignard« Dynamics of the contact line: contact angle
450 hysteresis »Phys. Rev. Lett. 1997, 79 (19), 3704–3707

451

452

7. Tables

Table 1: Main surface roughness parameters of the glass substrate measured by AFM in tapping mode on a 1 µm x 1 µm area.

8. Roughness parameters	9. Values (nm)
10. S_a	11. 0.43
12. S_q	13. 0.62
14. S_z	15. 7.8
16. S_v	4.2

Table 2: Different treated glass surfaces' wettability and the contact angle hysteresis before and after boiling experiments. The error bars are calculated using standard deviation over at least 5 measures.

	Before boiling experiments			**After boiling experiments**		
Surface treatment	**θ_r (°)**	**θ_a (°)**	**$H = \theta_a - \theta_r$ (°)**	**θ_r (°)**	**θ_a (°)**	**$H = \theta_a - \theta_r$ (°)**
Not grafted	0	0	0	8 ± 1.5	36.5 ± 1.9	28.5 ± 3.4
MPEGPTMS	33.5 ± 1.7	37.1 ± 0.3	3.6 ± 2	26.1 ± 1.9	37.1 ± 0.1	11 ± 2
AcOUTES	66.4 ± 1.2	88.3 ± 4.4	21.9 ± 5.6	46.8 ± 2.1	81.2 ± 4.1	34.4 ± 6.2
OTS	94.6 ± 0.8	113.9 ± 2.9	19.3 ± 3.7	90.2 ± 5.4	107.8 ± 1.2	17.6 ± 6.6

17. Figure captions

Figure 1

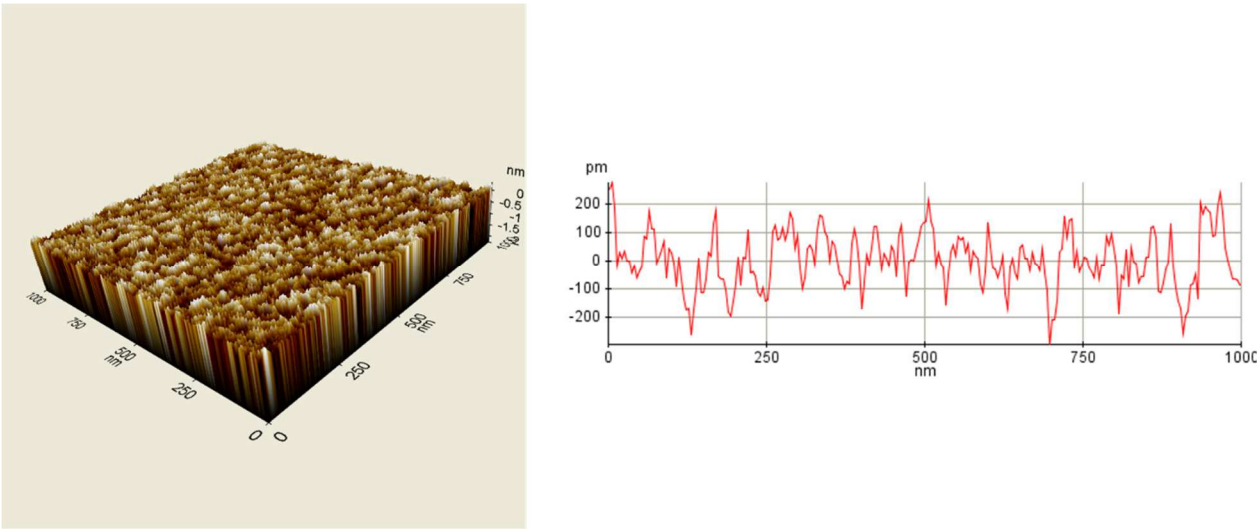

Figure 1: 3D view of the surface (left) and profile view (right) measured with AFM in tapping mode.

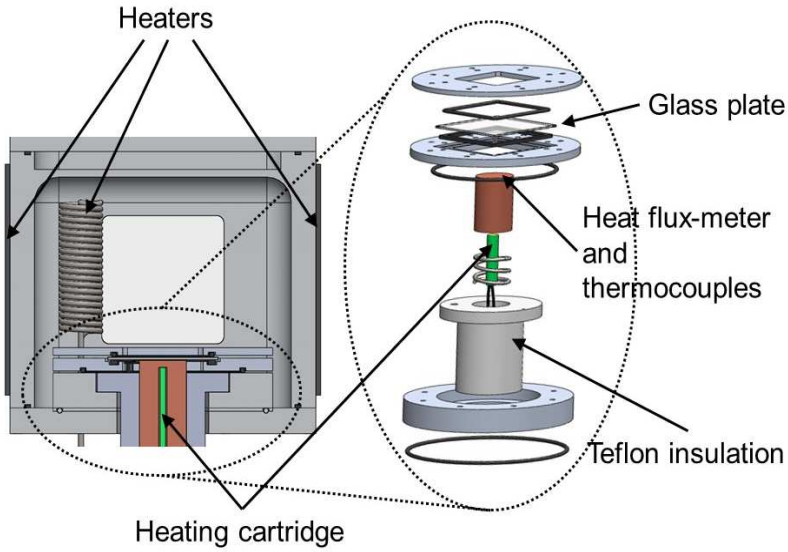

Figure 2: Schematic of the chamber. The glass plate, grafted with various silanes, is our studied surface.

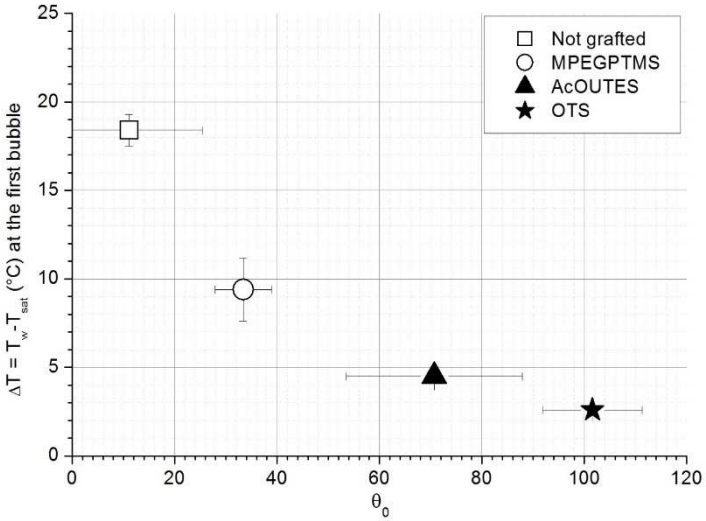

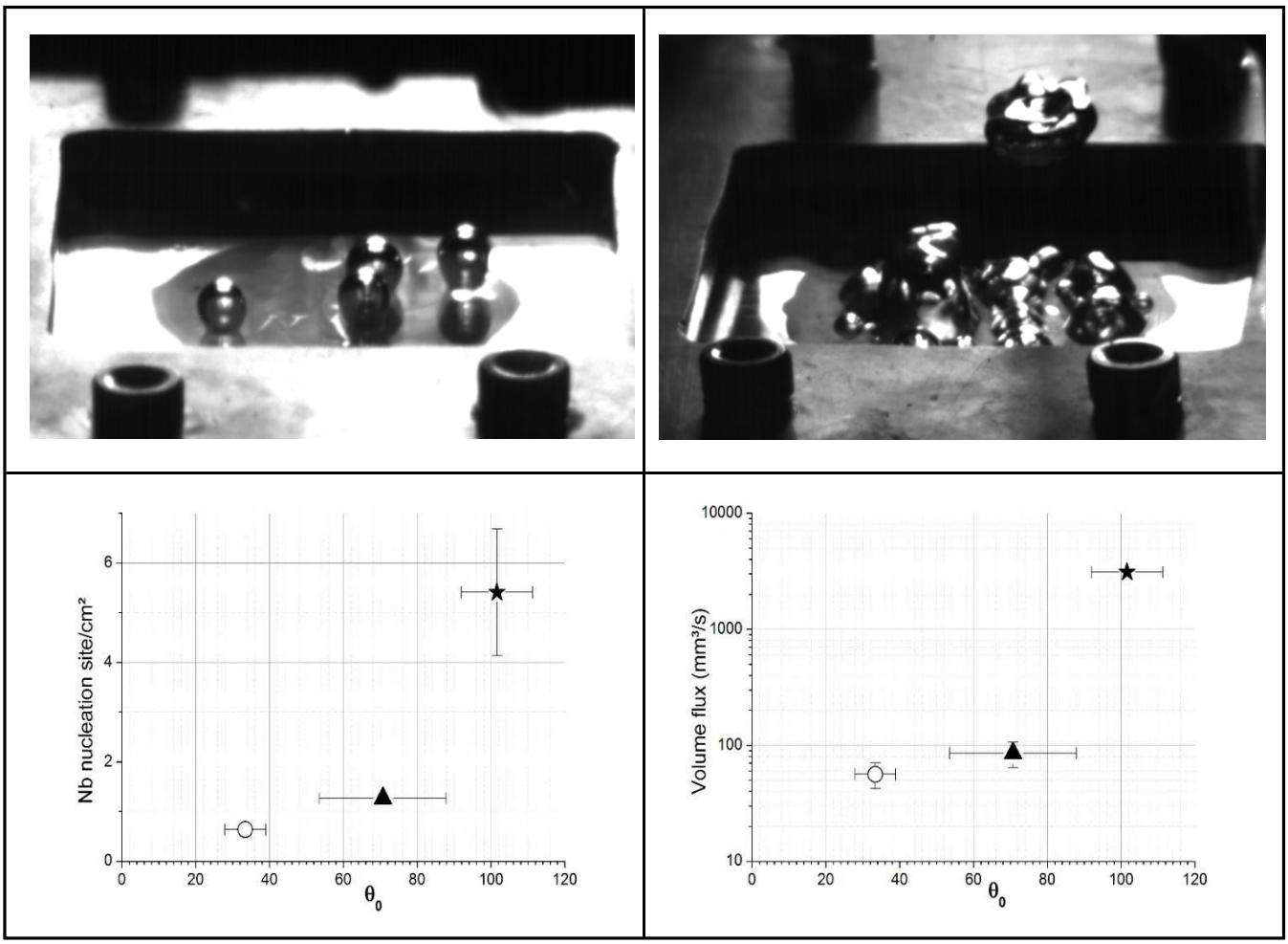

Figure 4: Comparison between surfaces boiling at the same heat flux (12kW/m²) on the smooth surfaces. Top: images from a tilted angle presenting the difference of boiling intensity on the surface (left: AcOUTES; right: OTS). The diameter of the heated disk is two centimeters. Bottom: quantification in terms of nucleation site density (left) and vapor volume flux (right) of the boiling process in function of the wettability. Symbols correspond to, from left to right, MPEGPTMS, AcOUTES and OTS.

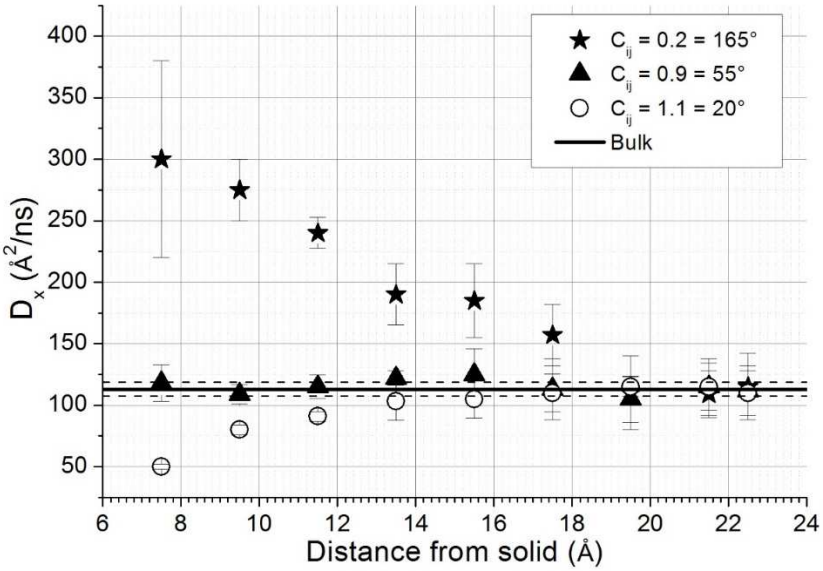

Figure 5: Diffusion constant versus the distance from the solid for three different coupling values. The coupling values 0.2, 0.9, and 1.1 correspond to a static contact angle of 165°, 55°, and 20°, respectively.

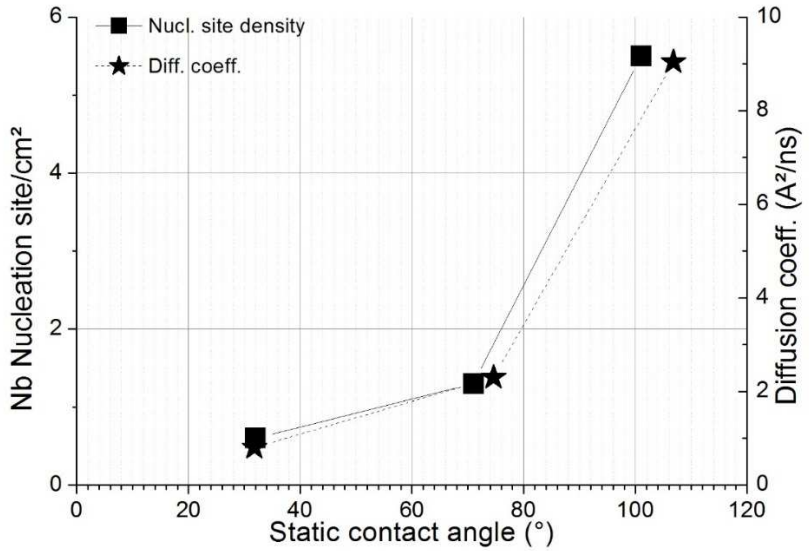

Figure 6: Nucleation site density (from our experiments) and diffusion coefficient (from molecular dynamics simulations) versus the static contact angle.

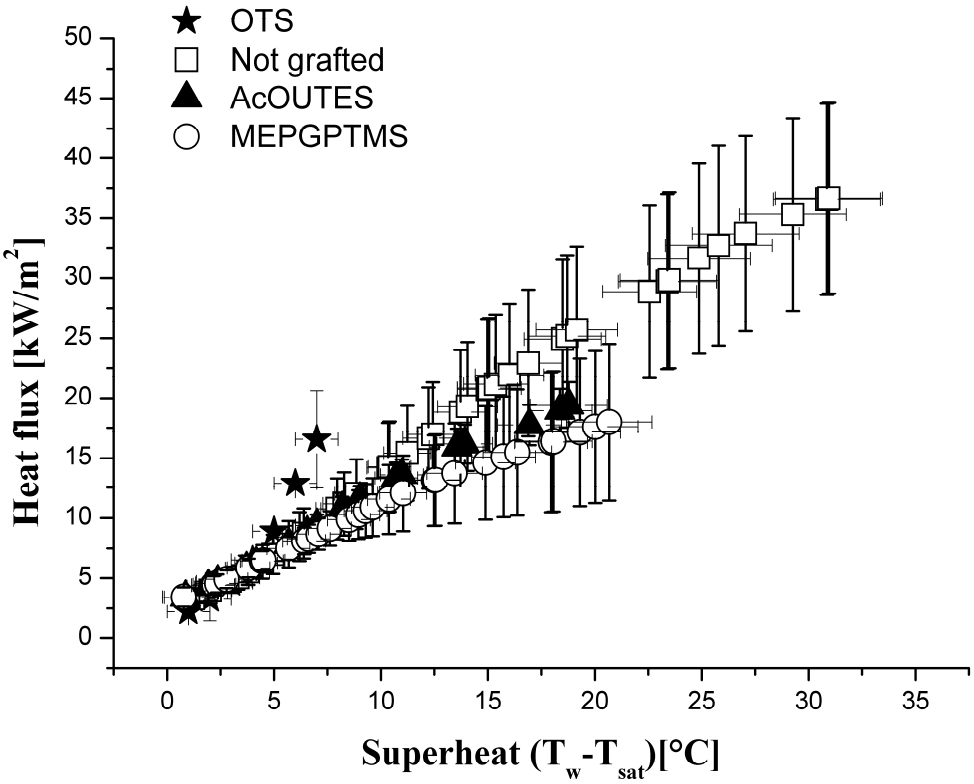

Figure 7: Boiling curves for the different surface treatments. Only the OTS case shows a change in the slope of the curve when boiling occurs.

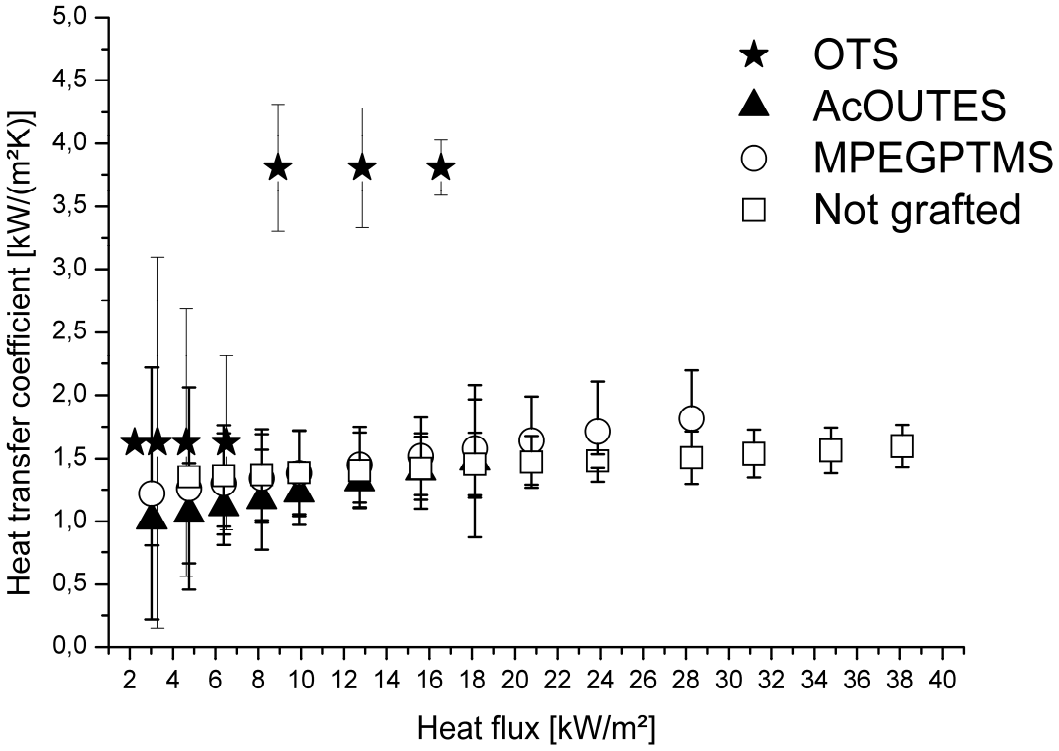

493

494 Figure 8: Heat transfer coefficient versus heat flux for each surface treatment.

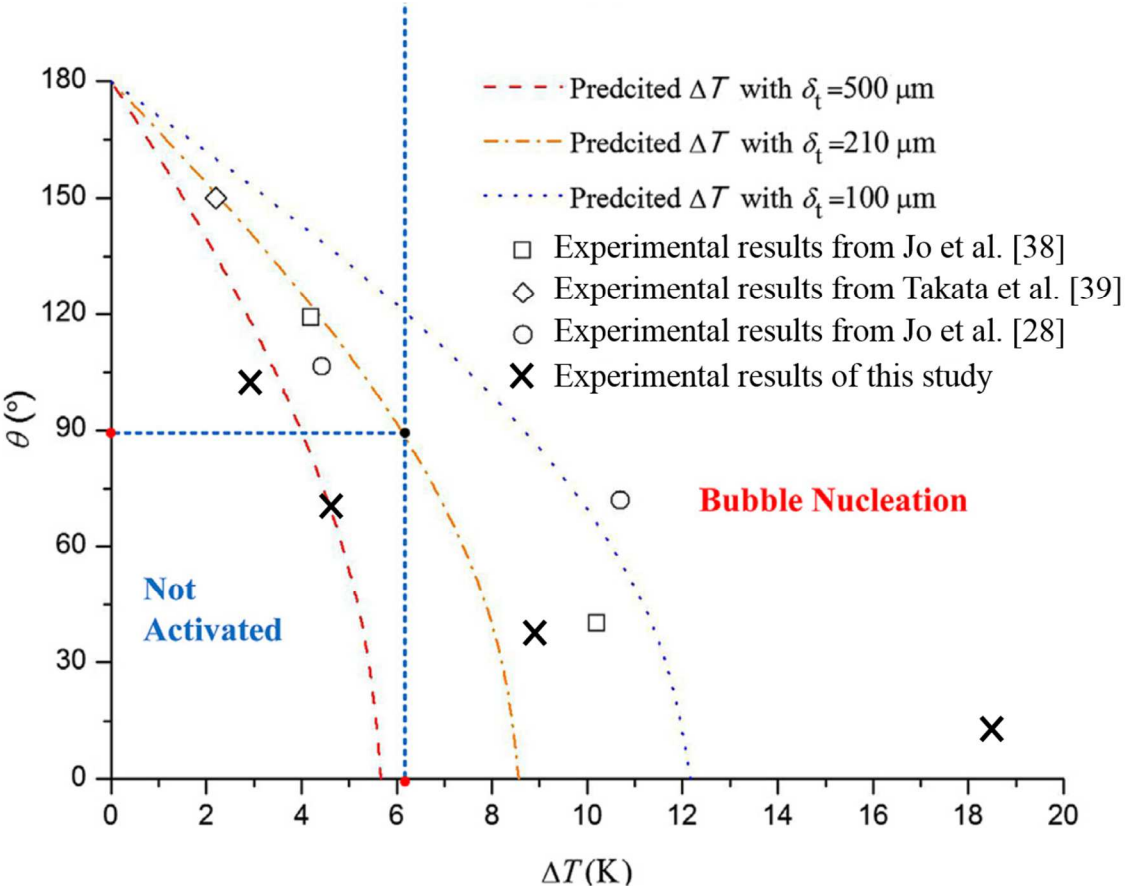

495

496 Figure 9: Comparison of the Jo et al.'s [28] predicted superheats as a function of contact angle for
497 different thermal boundary layer thicknesses with different experiments and with the experiment
498 results of this study.

499

500

18. Figures